substance: boron compounds with group I elements
property: properties of ternary boron-lithium compounds

$LiPt_3B$

Preparation and structure [87M].

Li_2Pt_3B (and Li_2Pd_3B): Ternary lithium borides of palladium and platinum with boron in octahedral coordination [97E].

Li_2Pd_3B

see Li_2Pt_3B [97E].

solid solution of Li in β-rhombohedral B

Interstitially doped β-rhombohedral boron (Li_xB_{105}), see LB III/41C "Boron"

$LiAlB_{14}$

Structure

The boron framework contains four B_{12} icosahedra and eight isolated B atoms in the unit cell. The icosahedra are centered at 0,0,0; 1/2,1/2,0; 0,0,1/2; 1/2,1/2,1/2 being oriented with one of their mirror planes parallel to the (100) plane. There are two kinds of intericosahedral B – B bonds. One of them is parallel to the *c*-axis and the other one parallel to the (110) planes thus leading to infinite chains of B_{12} icosahedra. All icosahedra are crystallographically equvalent, the isolated B atoms as well. Six apical atoms of an icosahedron are linked to those of neighboring icosahedra, the remaining six are linked via the isolated B atoms. The Li and Al atoms are accommodated in the large holes between the icosahedra.

lattice: orthorhombic; space group: D_{2h}^{28} – Imam [81H1].

lattice parameters

a	5.8469(9) Å	*T* = 300 K	Weissenberg and precession method	81H1
b	8.1429(8) Å			
c	10.3542(6) Å			

interatomic distances

(in Å)

d	2.28	Al – 12B	93W
	2.70	Li – 16B	
	2.923	Al – Al	
	3.361	Li – Li	

Comparison of the interatomic distances in $LiAlB_{14}$, $MgAlB_{14}$, Mg_2B_{14} and $NaB_{0.8}B_{14}$ [81H1].

Charge density distribution [83I].

Deformation of the electron density through one of the bisecting planes of the icosahedron in Fig. 1 [87H3].

Physical properties

Density of states calculation in Fig. 2 [91B, 94B].

energy gap
(in eV)

E_g	1.8	T = 300 K	extrapolated electroabsorption	88W1
	2.8		extrapolated electroabsorption	
	3.6		maximum photoconductivity	88W1, 86W
	1.18(2)	T = 300 K	(1a) indirect allowed interband or	93W
	1.20(2)		(1b) deep level to band	
	1.55(2)		(2) indirect allowed interband	
	1.57(2)		(3a1) $E \parallel a$, indirect allowed interband	
	1.78(2)		(3a2) $E \parallel a$, indirect allowed interband	
	1.86(1)		(3a3) $E \parallel a$, indirect allowed interband	
	1.54(2)		(3b1) $E \parallel c$, indirect allowed interband	
	1.94(1)		(3b2) $E \parallel c$, indirect allowed interband	
	1.95(2)		(4) indirect allowed interband	
	2.35(2)		(5) indirect allowed interband	
	2.51(1)		(6) indirect allowed interband	

(numbers in parentheses in column "remarks" correspond to the energies marked in Fig. 3)

$E_{g,ind}$	1.82	T = 300 K	single crystals (orientation not defined); optical absorption	81W2
	2.05	T = 300 K	maximum of photoconduction	81W2
	1.88		indirect	86W

Spectra of interband transitions in Fig. 3; optical absorption [93W], electroabsorption [88W1], photoconduction [86W].

For interband transitions see also [93W, 94W, 86W].

Temperature dependence of the absorption edge (absorption spectra at 22, 83 and 293 K) in Fig. 4 [93W].

Anisotropy of the absorption edge; absorption coefficient α vs. photon energy for $E \parallel a$ and $E \parallel c$ in Fig. 5 [93W].

Optical absorption spectra of $LiAlB_{14}$ (compared with $MgAlB_{14}$ and $ErAlB_{14}$)in particular in the range of the absorption edge in Fig. 6 [93W].

number of IR-active phonons (group theoretically determined)

B_{1u}	25	(assumed structure: 4 B_{12} icosahedra,	87H2
B_{2u}	27	8B atoms, 4M and 4M’ atoms)	
B_{3u}	21		

IR phonon resonance wavenumbers

(in cm^{-1})

v/*c*	703.2	*T* = 300 K	possibly double band	87H2
	738			
	753			
	758.7, 768.1		possibly double band	
	(777.6)			
	796.2			
	862.1			
	895.3, 910.8		strongest band, possibly double band	
	954.2		weak	
	1014.2			
	1237.6		strongest reflection and dispersion	
	1322.75			
	(1597)			

Optical reflectivity spectrum of $LiAlB_{14}$ (compared with $MgAlB_{14}$) in Fig. 7 [93W].

Optical absorption spectra of $LiAlB_{14}$ (compared with $ErAlB_{14}$) in the range of single atom vibrations in Fig. 8 [93W].

Optical absorption spectra of $LiAlB_{14}$ (compared with $MgAlB_{14}$, $ErAlB_{14}$) in the range of the phonon frequencies in Fig. 9 [93W].

For IR phonon spectra see also [87H1, 87W, 94W].

For the vibration spectrum of the Li atom in $LiAlB_{14}$ see also [94W].

IR absorption spectrum (poorly resolved) in [91G].

thermoelectric power

S	120(20) μV K^{-1}	*T* = 300 K		94W

density

d	2.46(2) g cm^{-3}	*T* = 300 K		93H
	2.46 g cm^{-3}	*T* = 300 K		81H2
	2.46(2) g cm^{-3}	*T* = 300 K		81H3

melting point

T_m	~2300 K		estimated	81H1
	< 1500°C			81H3

microhardness

(in kg mm^{-2})

H_K	2620	*T* = 300 K	1 N load, (010)	86W
	2955...2985		(001)	93H
	2470...2530		(010)	
	2620	*T* = 300 K	1 N load	81W1

LiBC

Completely intercalated heterographite

Space group: $P6_3/mmc$

Structure in Fig. 10 [95W].

Preparation (synthesized from the elements in sealed niobium ampoules at 770K and short annealing at 1770 K) and structure in [95W].

lattice parameters

a	2.7523(3) Å	*T* = 295K	X-ray diffraction	95W
c	7.058(2) Å			
c/a	2.564			

Electronic properties

Core-loss edges in Fig. 11 [97G].

energy gap

E_g	4.2 eV	calculated (INDO procedure)	95W
	2.5 eV	calculated (LMTO method)	

INDO is assumed to yield reliable, LMTO too small gaps [95W].

Optical properties

Stoichiometric crystals are red transparent; this confirms the semiconducting character [95W].

$LiBO_2$

Space group: $P2_1/c$

lattice parameters
(in Å)

a	5.845(1)	*T* = 300 K	X-ray diffraction	81W2
b	4.353(1)			
c	6.454(1)			
β	115.09(1)°			
V	148.724 $Å^3$			

Electron deformation density distribution in [81W2].

References:

81A Armstrong, D. R.: Proc. 7th Int. Symp. Boron, Borides and Related Compounds. Uppsala, Sweden, 1981; spec. issue of J. Less-Common Met. 82 (1981) 357.

81H1 Higashi, I.: J. Less-Common Met. 82 (1981) 317.

81H2 Hiebl, K., Rogl, P., Sienko, M.J.: J. Less-Common Met. 82 (1981) 201.

81H3 Higashi, I.: see [81A], p. 317.

81W1 Werheit, H., Higashi, I., preliminary results.

81W2 Will, G., Kirfel, A., Josten, B., Fröhlich, T.: J. Less-Common Met. 82 (1981) 255 (Proc. 7th Int. Symp. Boron, Borides and Rel. Compounds, Uppsala, Sweden, 1981).

81W3 Werheit, H., de Groot, K., Malkemper, W.: see [81A], p. 153.

83I Ito, T., Higashi, I.: Acta Crystallogr B 39 (1983) 239.

86W Werheit, H., Franz, R., Higashi, I.: J. Less-Common Met. 117 (1986) 169 (Proc. 8th Int. Symp. Boron, Borides, Carbides, Nitrides and Rel. Compounds, Tbilisi, Oct. 8 - 12, 1984).

87H1 Haupt, H., Werheit, H., Siejak, V., Gurin, V.N., Korsukova, M.M.: in: Proc. 9th Int. Symp. Boron, Borides and Rel. Compounds, University of Duisburg, Germany, Sept. 21 - 25, 1987, H. Werheit ed., University of Duisburg: Duisburg, 1987, p. 387.

87H2 Haupt, H., Werheit, H., Siejak, V., Kannengiesser, U., Higashi, I.: in: Proc. 9th Int. Symp. Boron, Borides and Rel. Compounds, University of Duisburg, Germany, Sept. 21 - 25, 1987, H. Werheit ed., University of Duisburg: Duisburg, 1987, p. 385.

87H3 Higashi, I., Ito, T.: in: Proc. 9th Int. Symp. Boron, Borides and Rel. Compounds, University of Duisburg, Germany, Sept. 21 - 25, 1987, H. Werheit ed., University of Duisburg: Duisburg, 1987, p. 41.

87M Mirgel, R., Jung, W.: in: Proc. 9th Int. Symp. Boron, Borides and Rel. Compounds, University of Duisburg, Germany, Sept. 21 - 25, 1987, H. Werheit ed., University of Duisburg: Duisburg, Germany, 1987, p. 285.

87W Werheit, H.: in: Proc. 9th Int. Symp. Boron, Borides and Rel. Compounds, University of Duisburg, Germany, Sept. 21 - 25, 1987, H. Werheit ed., University of Duisburg: Duisburg, 1987, p. 142.

88W1 Werheit, H., Kuhlmann, U., Tanaka, T.: (unpublished results).

88W2 Wood, C.: Rep. Prog. Phys. 51 (1988) 51.

91B Bullett, D.W.: AIP Conf. Proc. 231 (1991) 21, in: Boron-Rich Solids, Proc. 10th Int. Symp. Boron, Borides and Rel. Compounds, Albuquerque, NM 1990 (AIP Conf. Proc. 231), D. Emin, T.L. Aselage, A.C. Switendick, B. Morosin, C.L. Beckel ed., American Institute of Physics: New York, 1991, p. 21.

91G Golikova, O.A., Sokolov, A.P.: in: Boron-Rich Solids, Proc. 10th Int. Symp. Boron, Borides and Rel. Compounds, Albuquerque, NM 1990 (AIP Conf. Proc. 231), D. Emin, T.L. Aselage, A.C. Switendick, B. Morosin, C.L. Beckel ed., American Institute of Physics: New York, 1991, p. 347.

93H Hori, A., Kimura, K., Tada, T., Yamashita, H.: J. Non-Cryst. Solids 153&154 (1993) 308.

93W Werheit, H., Kuhlmann, U., Krach, G., Higashi, I., Lundström, T., Yu, Y.: J. Alloys Compounds 202 (1993) 269.

94B Bullett, D.W.: Proc. 11th Int. Symp. Boron, Borides and Rel. Compounds, Tsukuba, Japan, August 22 - 26, 1993, Jpn. J. Appl. Phys. Series 10 (1994), p. 31.

94W Werheit, H., Krach, G., Kuhlmann, U., Higashi, I., Lundström, T., Yu, Y.: Proc. 11th Int. Symp. Boron, Borides and Rel. Compounds, Tsukuba, Japan, August 22 - 26, 1993, Jpn. J. Appl. Phys. Series 10 (1994), p. 98.

95W Wörle, M., Nesper, R., Mair, G., Schwarz, M., v. Schneering, H.G.: Z. Anorg. Allg. Chem. 621 (1995) 1153.

97E Eibenstein, U., Jung, W.: J. Solid State Chem. 133 (1997) 21 (Proc. 12th Int. Symp. on Boron, Borides and Rel. Compounds, Baden, Austria, 1996).

97G Garvie, L.A.J., Buseck, P.R., Rez, P.:Characterization of beryllium-boron-bearing materials by parallel electron energy-loss spectroscopy (PEELS); J. Solid State Chem. 133 (1997) 347 (Proc. 12th Int. Symp. Boron, Borides and Rel. Compounds, Baden, Austria, 1996).

Fig. 1.

$LiAlB_{14}$. Deformation densities through one of the bisecting planes of the icosahedron. Contours at 0.05 $eÅ^{-3}$, negative contours dotted [87H3].

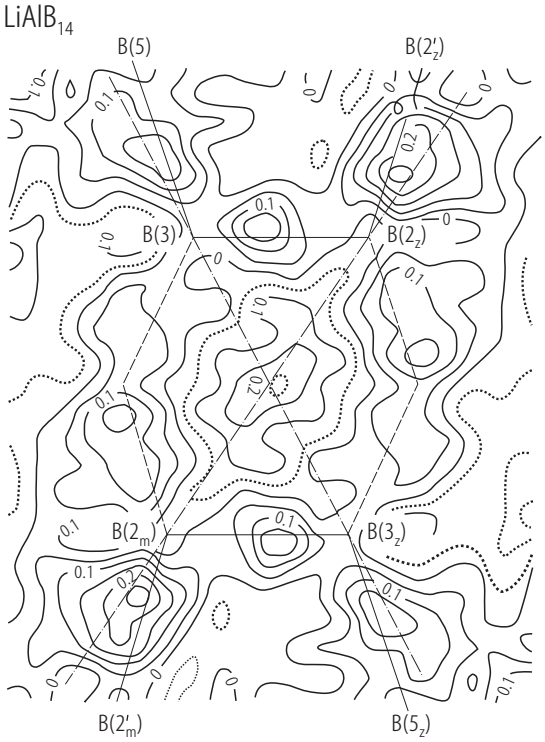

Fig. 2.

$LiAlB_{14}$. Calculated density of states for electrons [91B, 94B].

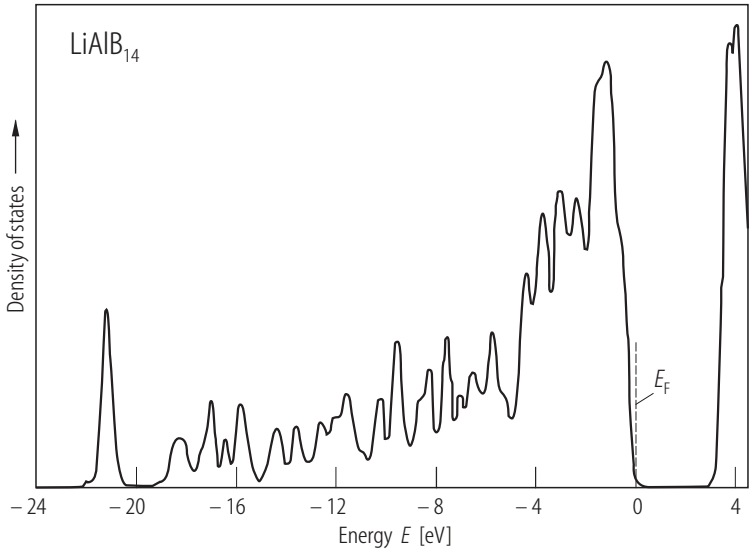

Fig. 3.

$LiAlB_{14}$. Spectra of interband transitions at 300 K. Triangles, electroabsorption [88W1], circles, photoconduction (two different samples) [86W]; vertical lines, transition energies determined from optical absorption (cp. table) [93W].

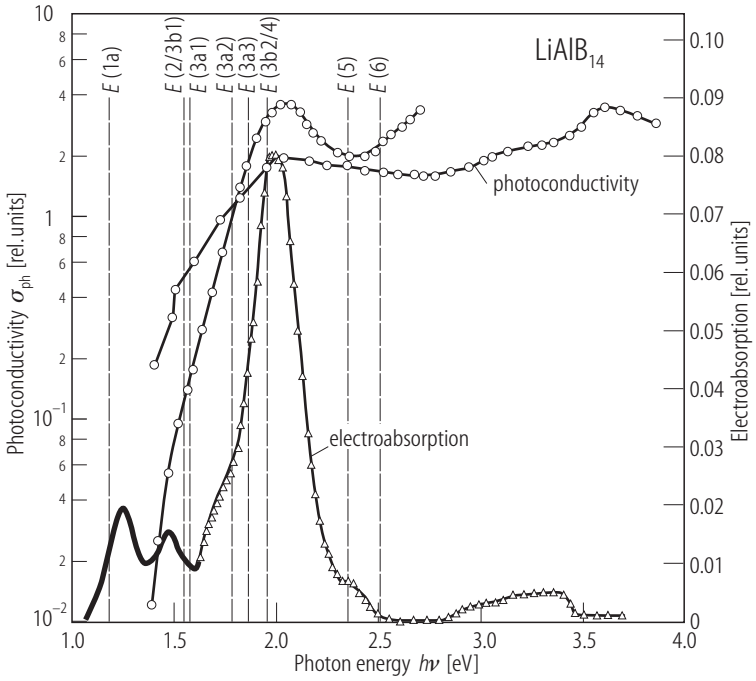

Fig. 4.

$LiAlB_{14}$. Temperature dependence of the absorption edge (absorption spectra at 22, 83 and 293 K) [93W].

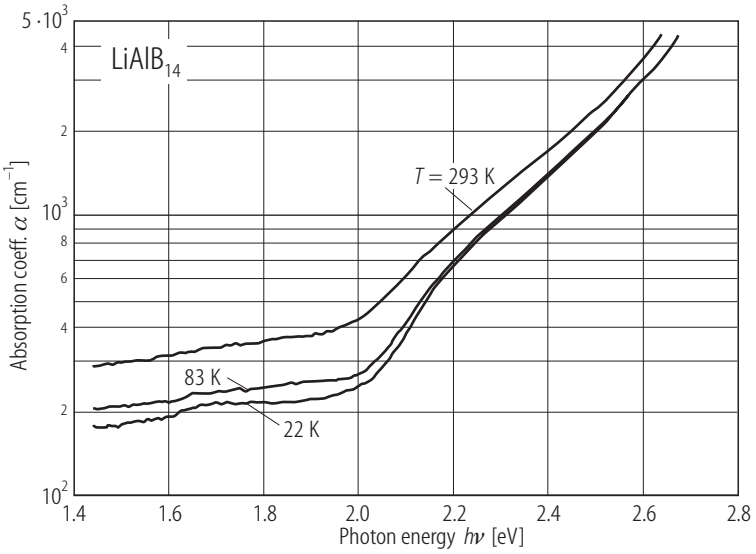

Fig. 5.

$LiAlB_{14}$. Anisotropy of the absorption edge; absorption coefficient α vs. photon energy for $E \parallel a$ and $E \parallel c$ at T = 293 K [93W].

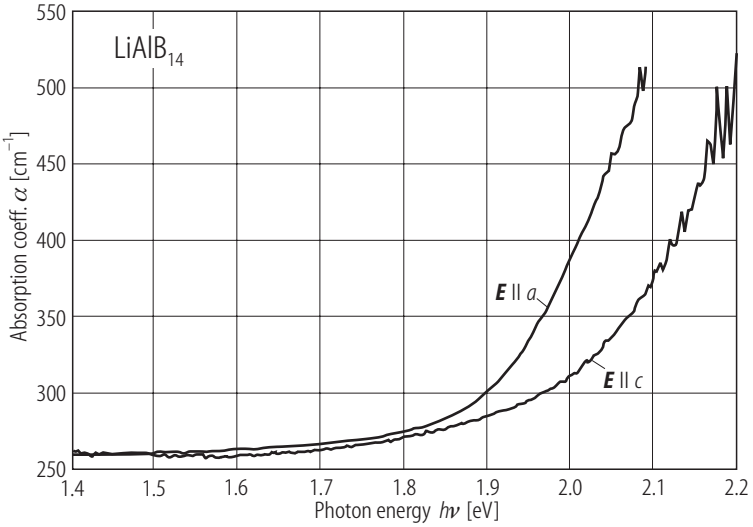

Fig. 6.

$MgAlB_{14}$ type orthorhombic structure group ($LiAlB_{14}$, $MgAlB_{14}$, $ErAlB_{14}$). Optical absorption spectra, in particular in the range of the absorption edge [93W].

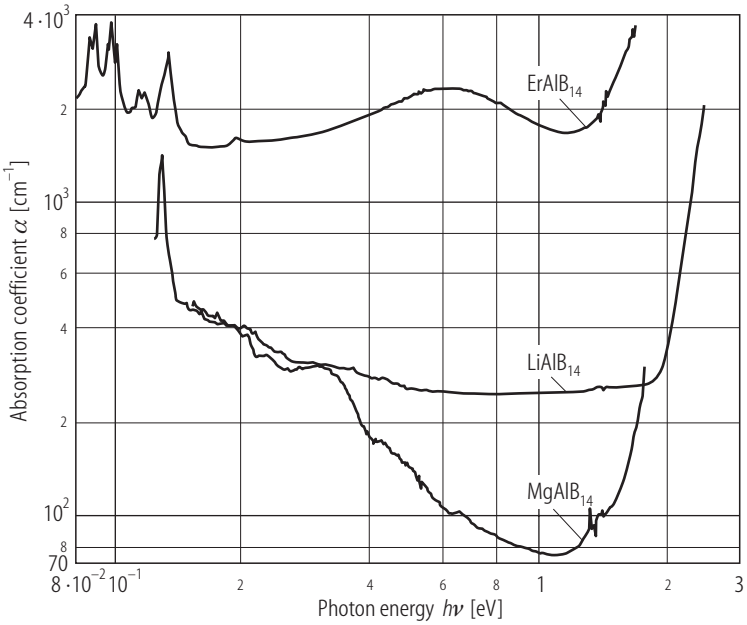

Fig. 7.

$MgAlB_{14}$ type orthorhombic structure group ($LiAlB_{14}$, $MgAlB_{14}$). Reflectivity spectra [93W].

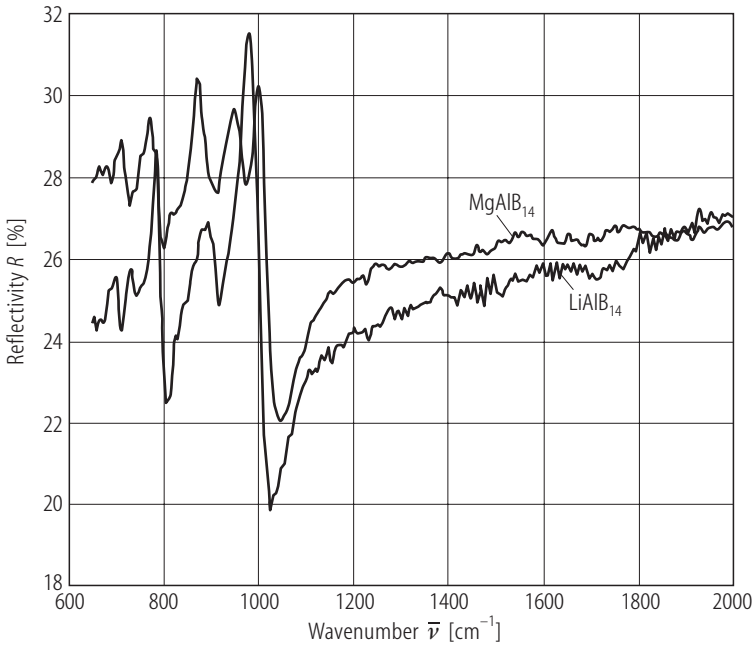

Fig. 8.

$MgAlB_{14}$ type orthorhombic structure group ($LiAlB_{14}$ (left ordinate), $ErAlB_{14}$ (right ordinate)). Optical absorption spectra in the range of single atom vibrations [93W].

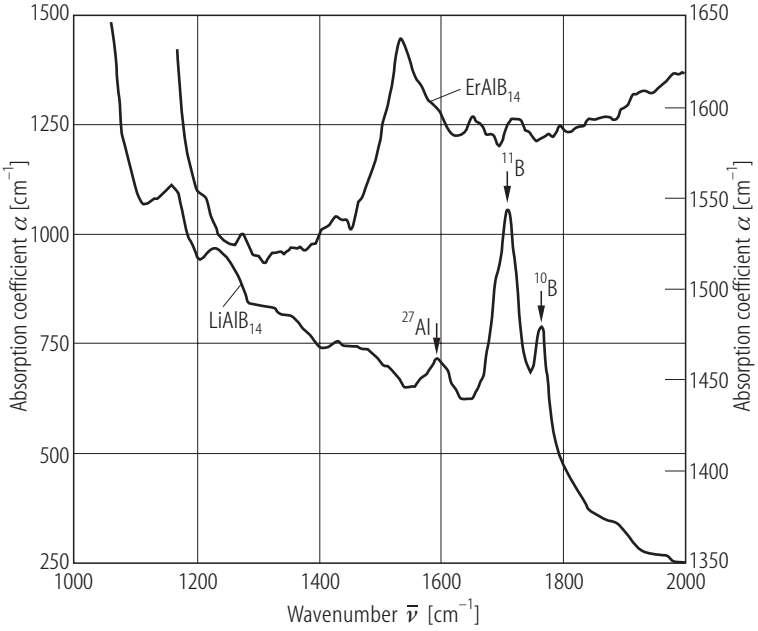

Fig. 9.

$MgAlB_{14}$ type orthorhombic structure group ($LiAlB_{14}$, $MgAlB_{14}$, $ErAlB_{14}$). Optical absorption spectra in the range of phonon frequencies [93W].

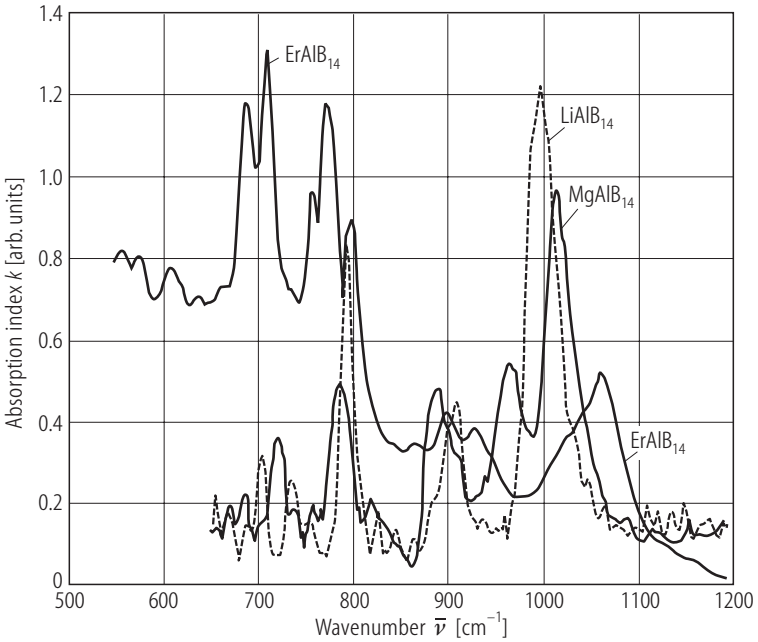

Fig. 10.

LiBC. Crystal structure. **(a)** View along the crystallographic *c* axis; **(b)** layers of the structure. Dark spheres, B atoms; light spheres, C atoms. The Li atoms are acccommodated at the corners of the trigonal prisms [95W].

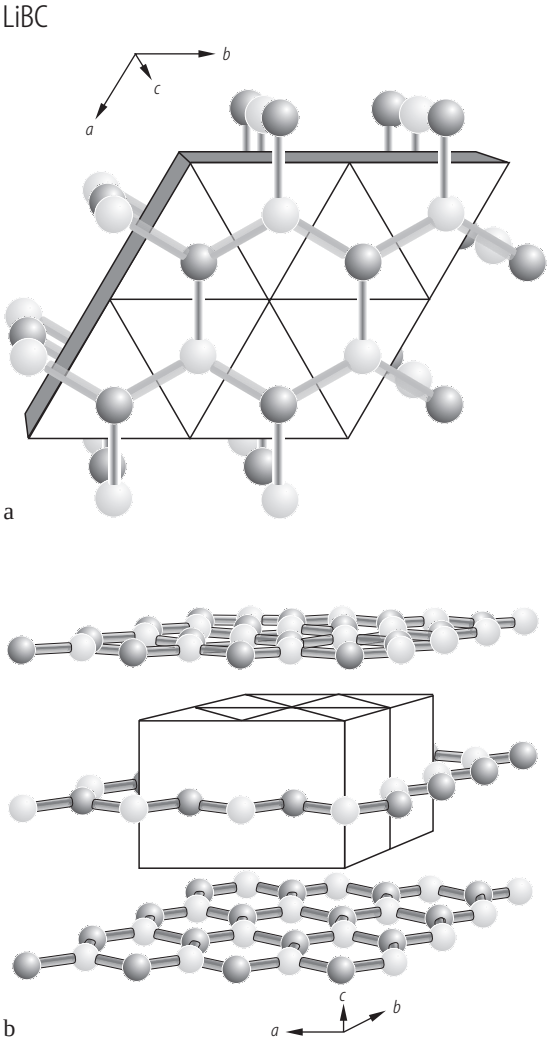

Fig. 11.

LiBC. Core loss spectrum. The K core-loss edges are a projection of the atom resolved, partial density of states of the conduction band representing the unoccupied p states for the inonized atom [97G].